2610–2623 *Nucleic Acids Research, 2011, Vol. 39, No. 7* *Published online 7 December 2010*
doi:10.1093/nar/gkq1215

Replication fork stalling by bulky DNA damage: localization at active origins and checkpoint modulation

Eugen C. Minca and David Kowalski*

Department of Cancer Biology, Roswell Park Cancer Institute, Buffalo, NY 14263, USA

Received January 21, 2010; Revised November 9, 2010; Accepted November 11, 2010

ABSTRACT

The integrity of the genome is threatened by DNA damage that blocks the progression of replication forks. Little is known about the genomic locations of replication fork stalling, and its determinants and consequences *in vivo*. Here we show that bulky DNA damaging agents induce localized fork stalling at yeast replication origins, and that localized stalling is dependent on proximal origin activity and is modulated by the intra–S–phase checkpoint. Fork stalling preceded the formation of sister chromatid junctions required for bypassing DNA damage. Despite DNA adduct formation, localized fork stalling was abrogated at an origin inactivated by a point mutation and prominent stalling was not detected at naturally-inactive origins in the replicon. The intra–S–phase checkpoint contributed to the high-level of fork stalling at early origins, while checkpoint inactivation led to initiation, localized stalling and chromatid joining at a late origin. Our results indicate that replication forks initially encountering a bulky DNA adduct exhibit a dual nature of stalling: a checkpoint-independent arrest that triggers sister chromatid junction formation, as well as a checkpoint-enhanced arrest at early origins that accompanies the repression of late origin firing. We propose that the initial checkpoint-enhanced arrest reflects events that facilitate fork resolution at subsequent lesions.

INTRODUCTION

Faithful duplication of DNA is challenged by natural or abnormal obstacles on the template that can block the progression of replication forks. Stalled forks represent potentially hazardous structures that can be subject to replisome collapse or DNA breakage and can be a source of harmful genome rearrangements. Mechanisms that allow the stabilization and the timely restart of stalled replication forks are essential for the maintenance of genome stability and cell survival (1,2). Although of major research interest, the investigation of these mechanisms is difficult due to the transitory temporal and spatial nature of the stalled replication forks.

Discrete pausing of replication fork progression occurs in normal conditions at various specific genomic sites, such as the rDNA or centromeric DNA, and is caused by the collision of forks with proteins tightly bound to DNA. The protein–induced replication–fork barriers are regulated by several replisome components. While some factors promote the fork pause, other proteins disrupt protein–DNA interactions and relieve the fork block (3,4). Specific fork pauses have been observed at replication origin sites that are either naturally-inactive or rendered defective by the mutation of a replication initiation gene (5,6). In this case, the fork pausing is caused by collision with a replication initiation complex bound to DNA in the absence of origin firing. The programmed replication fork pausing at protein–blocked sites does not result in intra–S–phase checkpoint activation and does not appear to require DNA recombination for fork restart in budding yeast (4).

Unlike naturally occurring protein blocks, DNA lesions obstructing replication forks induce activation of intra–S–phase checkpoint and fork restart mechanisms. The intra–S–phase checkpoint delays the mitotic entry and inhibits late–origin firing (7). The Mec1 sensor kinase is essential for checkpoint activation and for stabilizing stalled replication forks after its recruitment along with the Ddc1/Mec3/Rad17 checkpoint clamp (8). Ddc1 and other factors stimulate the Mec1 activity, which, through mediators like Mrc1 and Tof1, promotes checkpoint activation (9,10). Concomitantly, replication is restarted at stalled forks through DNA damage bypass mechanisms (11). The contribution of the intra–S–phase checkpoint

*To whom correspondence should be addressed. Tel: +716 845 4462; Fax: +716 845 4928; Email: david.kowalski@roswellpark.org; kowalsk@buffalo.edu

in regulating the replication fork stalling at DNA damage sites is not fully understood.

Replication forks are required for S–phase checkpoint activation (12) and are established at multiple origin sites (ORI) bound by the origin recognition complex (ORC) and other initiation factors (13). In *Saccharomyces cerevisiae*, an essential consensus DNA element within each autonomously replicating sequence (ARS) binds ORC and is required for chromosomal origin function (14). Most, but not all, ARSs function as active chromosomal origins, each with a specific activation timing, which can be in early, mid or late S phase (15). Despite containing the origin–specific DNA elements and initiating replication in plasmids, some ARSs are naturally inactive as chromosomal origins (16).

Earlier we found that DNA-alkylating agent adozelesin induces localized stalling of replication forks at an active early origin in budding yeast cells (17). Fork stalling at the origin was observed as an intense, discrete DNA spot following 2D–gel analysis of replication intermediates from asynchronous cells damaged in all phases of the cell cycle. How DNA damage affects the replisome progression may depend on the nature of the lesion. Methyl–methane-sulfonate (MMS) and UV radiation, frequently used to study the effects of DNA damage, induce small–sized, randomly–distributed lesions that slow down the rate of fork movement (18,19). However, localized fork stalling has not been directly observed (19–22). DNA damage caused by bulky adducts has not been extensively tested. Adozelesin, a member of the cyclopropylpyrroloindole family of compounds, forms bulky adducts in the DNA minor groove (23) and has specificity for AT–rich DNA sequences (24). Recently we found that factors involved in error-free DNA damage bypass and homologous recombination mediate the formation of sister chromatid junctions at replication forks stalled by adozelesin (25). Still, many aspects about the localized fork stalling identified earlier (17) remained unclear, such as the origin of the stalled forks, the existence of localized stalling caused by different alkylating agents or at other genomic loci, and the possible influence of S-phase checkpoint regulation.

In the present work we investigated the determinants of localized replication fork stalling in budding yeast, using synchronized cells damaged specifically in S phase by adozelesin or 4–nitroquinoline oxide (4NQO). We found that bulky DNA lesions induced fork stalling localized at a variety of replication origins, and that localized fork stalling was dependent on proximal origin activity and was checkpoint modulated. These and other findings indicate a dual nature of stalling replication forks upon initially encountering a bulky DNA adduct at active origins: a checkpoint-independent arrest that triggers formation of sister chromatid junctions, and an enhancement of fork arrest at early origins induced by the S-phase checkpoint, which also represses late origin firing and is proposed to facilitate fork resolution at subsequent lesions.

MATERIALS AND METHODS

Yeast strains

The wild–type (WT) strain used in this study was a *bar1::LEU2* version of BY4741 (*MATa his3Δ1 leu2Δ0 met15Δ0 ura3Δ0*). *ARS305*–b5c7 (26) and *mec1*–100 (27) isogenic derivatives were constructed using standard 2–step gene replacement protocols and confirmed by DNA sequencing. The plasmid containing the *mec1*–100 allele was a kind gift from M. Longhese. G1–synchronization was accomplished with 150 nM α–factor (Invitrogen) for 2.5 h at 25°C. Treatments with adozelesin (U–73 975; gift of T. Beerman), MMS and 4NQO (Sigma) were also performed at 25°C.

Flow cytometry

For flow cytometry analysis, cells fixed in 70% ethanol were washed with 50 mM Na citrate pH 7.0, resuspended in the same buffer containing 100 μg/ml of RNaseA and incubated for 16 h at 37°C. Proteinase K was added to 300 μg/ml. Cells were incubated for 2 h at 37°C, stained with 1 μM Sytox Green (Molecular Probes), sonicated and analyzed on a FACScan (Becton Dickinson).

2D–gel analysis of replication intermediates

Genomic DNA from 10^9 cells was isolated by CsCl gradient centrifugation, followed by restriction endonuclease digestion and analyzed by 2D–gel electrophoresis as described previously (26). Restriction digestion was performed with *Eco*RI/*Fsp*I for all experiments and with *Pst*I and *Stu*I/*Pml*I for that described in Figure 3. The DNA probes used for ^{32}P–labelling and hybridization were created by PCR using oligonucleotides with sequences available upon request. The loaded DNA amount and the exposure time were equal for all the samples analyzed in the same experiment. The radioactive signals were detected using a STORM PhosphorImager. The resulting images were analyzed and signal intensities were determined using ImageQuant software (Molecular Dynamics).

RESULTS

Bulky DNA damage induces localized fork stalling and sister chromatid junctions at early replication origins

In a previous report we showed that exposure of asynchronous budding yeast cells to a bulky DNA alkylating agent, adozelesin, induces replication fork stalling predominantly at a site mapping to an early-firing origin, ORI305 (17). The studies were subject to experimental limitations of using asynchronous cells damaged in all phases of the cell cycle, which may have contributed to reduced origin activity. One unclear aspect is whether the stalled fork originated from active ORI305 itself or from a neighboring origin and passively replicated ORI305. To address this issue, we used G1–blocked cells released synchronously into S phase in the presence of adozelesin and analyzed replication intermediates by 2D–gel electrophoresis. The DNA structures and the

signals detected by 2D–gel analysis in the two distinct possibilities of stalling, involving a fork generated at either a proximal origin or a distal origin, are modeled in Figure 1. If the stalling involves forks generated at a distal origin (Figure 1A), then the result is the formation of an early–Y arc, and a prominent fork accumulation signal at the site of DNA damage. In contrast, if the stalling is localized at an active origin, involving forks generated proximally (Figure 1B), there is no early–Y arc accompanying the prominent fork stalling signal at the DNA lesion. Instead, a high-rising bubble arc forms indicating that the origin is active. In both cases, a late–Y arc would form if the fork block was removed and replication resumed.

To distinguish between these possibilities, we initially examined three genomic loci containing early origins: ORI305, ORI508 and ORI1014 present on chromosomes III, V and X, respectively. All origins were centrally located in restriction enzyme fragments of chromosomal DNA (Figure 2, maps and sizes) in order to maximize detection of origin activity in the bubble arc as well as the formation of an early–Y arc. Schematic diagrams of the resolved replication intermediates in the presence and absence of DNA damage are shown in Figure 2D. In control experiments with haploid cells (1C DNA content) released from the G1 block into an unperturbed S phase, DNA replication initiated by 30 min, with a significant subpopulation showing DNA duplication at 60 min, as indicated by the 2C DNA–content peak on the flow–cytometry profile (Figure 2A). The early origins showed an intense bubble arc indicating strong firing at 30 min, which progressively decreased at 45 and 60 min (Figure 2A). Faint X-DNA signals visible at 30 min represent hemicatenane structures that form during normal replication (21). Clearing of the arc signals by 60 min indicates the completion of replication in the DNA fragments analyzed.

When cells were released from the G1 block into S phase in the presence of adozelesin, DNA replication initiated with similar timing as in the absence of damage and the activity of early origins reached a maximum at 30 min. However, the DNA damaging agent induced an accumulation of cells in S phase with a DNA content intermediate between 1C and 2C at 45 and 60 min as well as strong and discrete fork–stalling signals at the peak of the Y arc, mapping to the three centrally–located origin sites (Figure 2B). Minor fork stalling signals were also detected on the late–Y arc. Localized

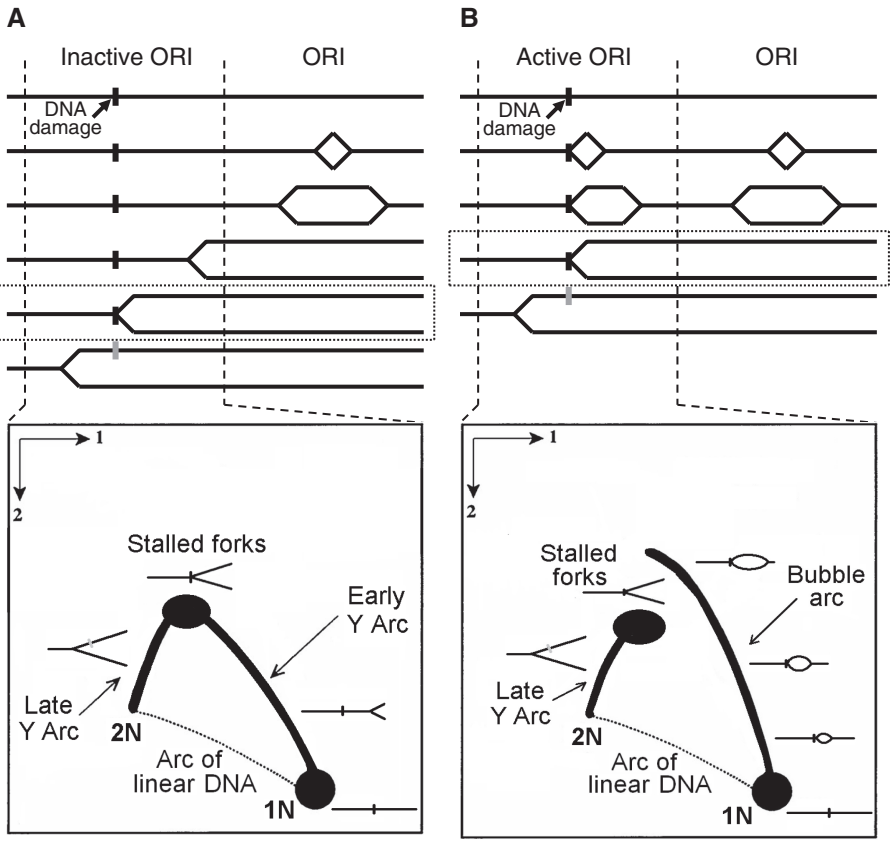

Figure 1. Theoretical DNA structures and 2D–gel signals expected upon localized stalling of replication forks generated at a proximal origin or a distal origin. The replication forks stalled by DNA damage at an inactive origin site are generated at a distal origin (**A**). The stalling results in the formation of an early–Y arc, and a prominent fork accumulation signal at the stalling site. In contrast, the localized stalling of replication forks generated proximally at an active origin (**B**) results in the absence of an early–Y arc and the formation of a high rising bubble arc, along with a strong fork stalling signal. In both cases, once the DNA lesion is repaired or bypassed and replication resumes, nearly fully replicated fragments are expected to form a late–Y arc ending in a virtual 2N spot of structures with twice the original amount of DNA, while the unreplicated or fully replicated linear fragments migrate at the 1N spot.

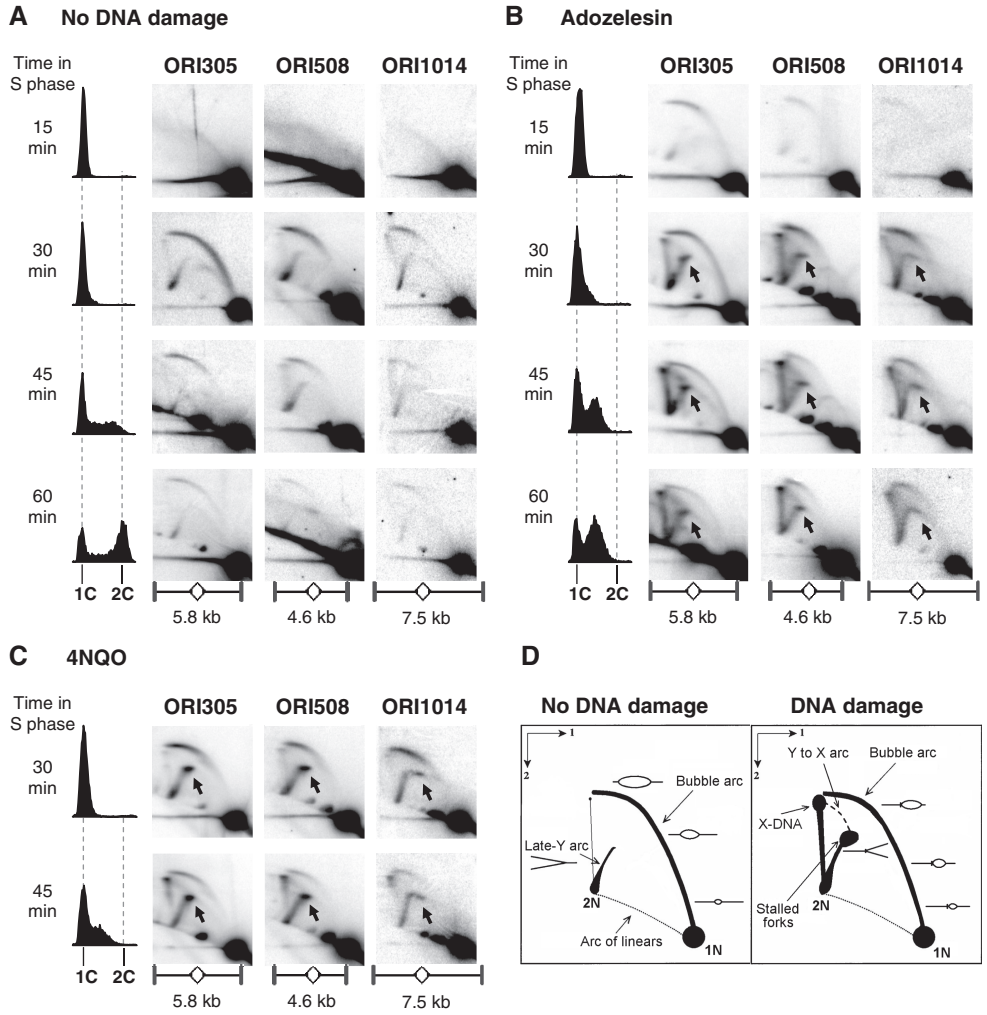

Figure 2. Replication forks stall at early–firing origins in the presence of bulky DNA damage in S phase. G1–synchronized WT cells were released into S phase without DNA damaging agents (**A**) or in the presence of 1 μM adozelesin (**B**) or 0.15 μg/ml 4NQO (**C**). Samples were collected at the indicated time points post-release for 2D-gel electrophoresis and flow–cytometry analysis of DNA content. Replication intermediates were analyzed at three different regions encompassing early–firing origins ORI305, ORI508 and ORI1014 and were schematically represented in panel (**D**). The arrows in (B, C) indicate the major fork–stalling signals induced by adozelesin and 4NQO at the origins. Results for MMS–treated cells are shown in Supplementary Figure S1.

fork stalling at the origin persisted up to 60 min, as did all other replication intermediates, indicating a general slowdown in fork progression. Importantly, the lack of a well-defined, early–Y arc at 30 min, when stalled forks were first detected, and the presence of a bubble arc, rule out passive replication from adjacent distal origins (Figure 1A) and indicate that the localized stalling involves forks generated at a proximal early origin (Figure 1B), in all three cases tested.

A well-defined, early–Y arc signal arose at a later time during the release into S phase (Figure 2B, 45 min). However, it was faint relative to the other replication signals, reflecting a low level of passive replication occurring in a minority of cells in which the origin was inactive.

In contrast to the results obtained using adozelesin, localized fork stalling was not observed following DNA damage by MMS (Supplementary Figure S1) (20,21) or UV radiation (19,22). This could be due to particular properties of the damaging agent and/or locus, or to differences in the mechanism for the sensing, repair or bypass of bulky DNA adducts.

To investigate whether a different DNA alkylating agent induces localized replication fork stalling, we tested the effect of 4NQO, which also forms bulky adducts in the DNA minor groove but, unlike adozelesin, has no described sequence specificity. When G1–blocked cells were released in S phase in the presence of 4NQO for 30 and 45 min, we observed a similar localized fork stalling at early origins ORI305, ORI508 and ORI1014 (Figure 2C). The stalled forks, first detected at 30 min, were accompanied by a bubble arc, lacked an early–Y arc, and were associated with the accumulation of cells with incompletely replicated DNA. These results, together with those obtained using adozelesin, indicate that the localized fork stalling is not confined to a particular origin or bulky damaging agent, but occurs at several active early origins during exposure to different bulky

DNA alkylating compounds in S phase, and involves forks generated at the proximal origin.

The fork stalling induced by adozelesin, first detected at 30 min (Figure 2B), preceded an increase in the levels of X–shaped DNA structures (Figure 2D, DNA damage), which are comprised of fully duplicated DNA fragments containing junctions between sister chromatids (28). These structures were not originally observed at ORI305 (17), where affinity chromatography was used for the enrichment of replication intermediates containing ssDNA (29). Recently we found that adozelesin-induced sister chromatid junctions lack detectable ssDNA and are formed through recombination-mediated bypass of DNA damage (25). The Y to X arc, first seen at 45 min (Figure 2B), connects the fork stalling signal to the most intense portion of the sister chromatid junction signal, and is comprised of elongating structures generated following the bypass of stalling lesions to form fully duplicated DNA with sister chromatid junctions (25). Less intense portions of the chromatid junction signal were associated with minor stalling signals present on the late–Y arc. As in the case of adozelesin, the fork stalling induced by 4NQO at 30 min preceded the formation of both the sister chromatid junctions and the Y to X arc at 45 min (Figure 2C). Thus, localized fork stalling induced at the origin by bulky alkylating agents is accompanied by, and precedes, the formation of sister chromatid junctions.

DNA damage–induced stalling affects newly–created replication forks emanating from the origin in either direction

The results presented above indicate that the localized stalling induced by DNA damage at active origins involves forks formed within the origin, as opposed to forks generated elsewhere that passively replicate the origin region. Stalling signals at active, bidirectional origins located in the center of the restriction fragments analyzed could be generated by forks arrested in a specific direction or in either direction, i.e. randomly. To distinguish between these possibilities, we used two different restriction digestions that place the ORI305 and ORI508 initiation sites on either side in relation to the center of the genomic DNA fragments (Figure 3). Stalling of forks moving in a specific direction from the origin would generate a stalling signal on the early–Y arc of only one off–centered digest. Stalling of forks moving in either direction from the origin would result in stalling signals on the early–Y arcs of both off–centered digests. During 4NQO–perturbed S phase, we detected fork stalling signals on the early–Y arcs of both off–centered digests

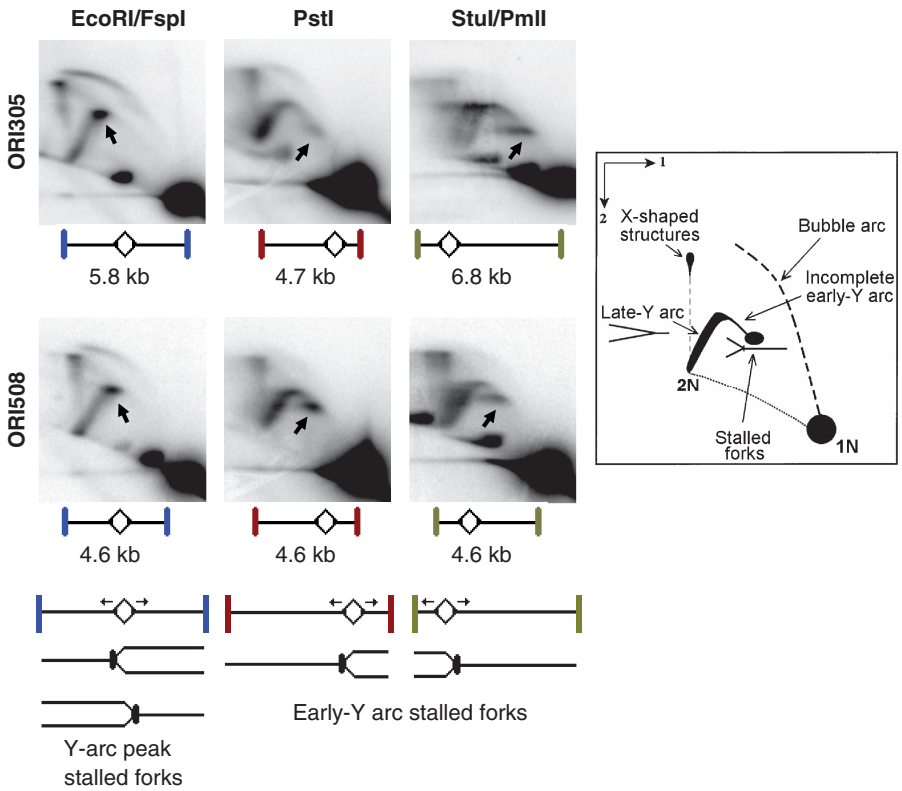

Figure 3. Replication fork stalling occurs in either direction at active origins. G1–synchronized WT cells were released into S phase in the presence of 0.15 μg/ml 4NQO. Samples were collected at 45 min post-release for 2D–gel electrophoresis. Replication intermediates were analyzed at ORI305 and ORI508 in the three alternative restriction digestion fragments indicated by the different colored bars. The relative position of the origin in each fragment is indicated by the diamond shape. The fork–stalling signal is indicated by arrows. Stalling–signal intermediates are schematically represented for each digest. Relevant signals observed in the presence of DNA damage are represented in the diagram. The bubble arc arising from an origin near the end of a DNA fragment is expected to be reduced in intensity and length and is schematized by a dotted line. Results for ORI607 and ORI306 are shown in Supplementary Figure S2.

at ORI305 and ORI508 (Figure 3). We also observed discrete 4NQO–induced fork stalling on the early–Y arc mapping to two additional early replication origins, ORI607 (on chromosome VI) and ORI306 (adjacent and distal to ORI305 on chromosome III) (Supplementary Figure S2). In every case, the early–Y arc was interrupted by the fork stalling signal with no intermediates between the latter and the non-replicating DNA in the 1N spot, confirming that the stalled forks were formed within each of the origins analyzed and not incoming from distal origins. These results indicate that the DNA damage–induced stalling involves newly–created replication forks that emanate from the origin and travel in either direction.

Localized fork stalling is dependent on proximal origin activity

The previous results show that bulky DNA damage leads to localized stalling of newly-created forks at active replication origins. We were interested in testing whether localized fork stalling is dependent on proximal origin activity. In the absence of proximal origin activity, a replication fork from a distal origin at an adjacent locus in the chromosome would be expected to stall at a DNA lesion at an inactive origin, as illustrated earlier in Figure 1A. To test the dependence on proximal origin activity, we used a yeast strain in which the origin activity of ORI305 was inactivated by a *cis*-acting point mutation in the ARS consensus element required for its function (*ARS305*–b5c7 derivative) (26). A single base mutation in the DNA sequence would not be expected to significantly influence the reactivity with alkylating agents. During the release of G1–blocked mutant cells into S phase in the absence of DNA damage, 2D–gel analysis of replication intermediates at inactive ORI305 revealed no strong bubble arc and an intense complete Y arc, i.e. early– and late–Y signals (Figure 4A). The presence of an intense early–Y arc indicates that

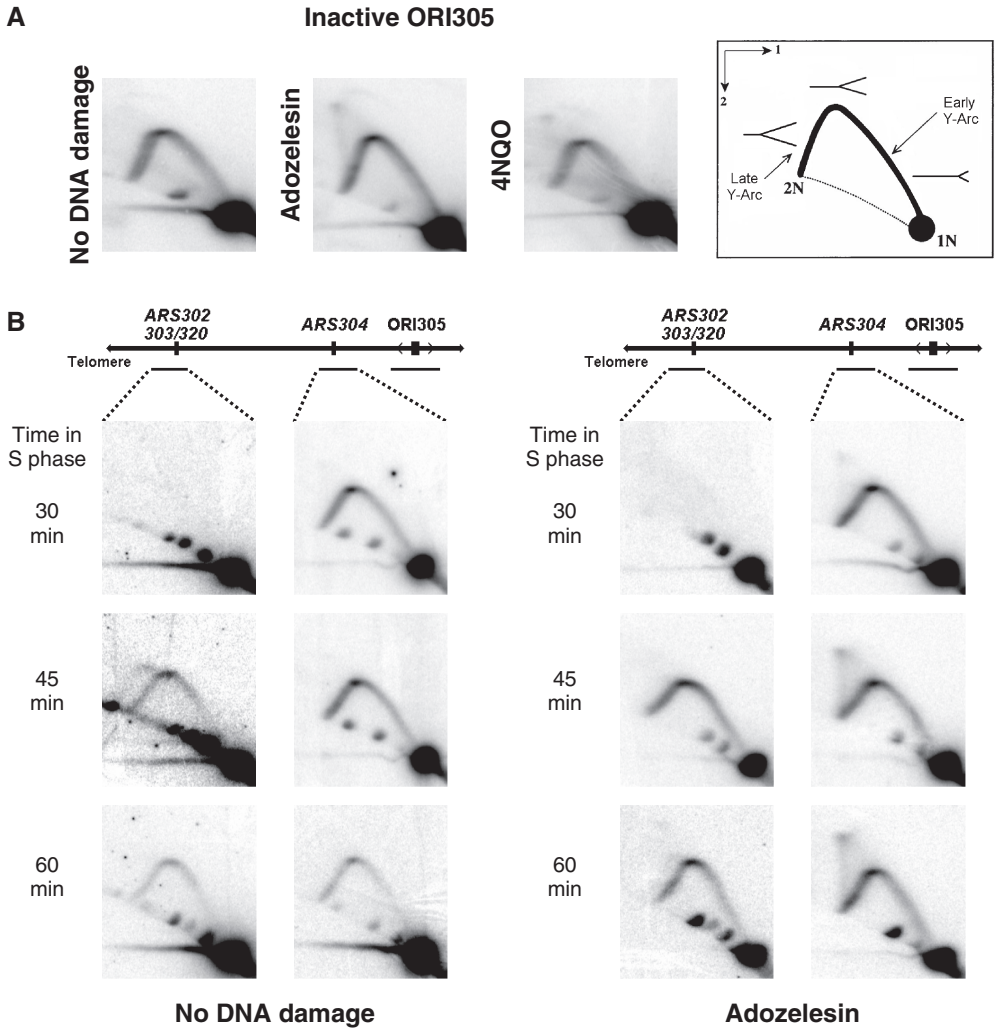

Figure 4. Localized replication fork stalling requires proximal origin activity. (**A**) G1–synchronized *ARS305*-b5c7 mutant cells were released into S phase without DNA damaging agents or in the presence of 1 μM adozelesin or 0.15 μg/ml 4NQO. Samples were collected at 45 min post–release for 2D–gel analysis of replication intermediates at the inactivated ORI305 locus. (**B**) G1–synchronized WT cells were released into S phase without DNA damaging agents or in the presence of 1 μM adozelesin. Samples were collected at the indicated time points post-release for 2D-gel analysis of replication intermediates at two regions encompassing the naturally-inactive *ARS304* and *ARS302*/*303*/*320* situated adjacent to, and on the telomeric side of, ORI305 on chromosome III (map).

replication was predominantly passive, originating from a centromere-proximal origin, such as the adjacent ORI306 (16), as there are no active origins between ORI305 and the telomere (Figure 4B, map). Upon release into S phase in the presence of adozelesin or 4NQO, the replication intermediates at inactive ORI305 were essentially unchanged compared to those seen in the absence of DNA damage. Unlike the active ORI305, the inactivated origin was replicated passively from a distal origin and showed no detectable damage–induced fork stalling signal at the peak of the Y arc (Figure 4A).

While the original studies on the *ARS305*–b5c7 derivative showed no chromosomal origin activity in asynchronous cells (26), the origin functioned at low efficiency in the different strain and conditions used here. Upon close inspection of Figure 4A, a faint bubble arc signal can be seen, both in the presence and absence of DNA damage. At the correspondingly low level of origin proximal forks generated, localized fork stalling is not detectable, and if present at a low level, would be obscured by the abundant passive replication by forks from an external origin. However, a low level of X-structures dependent on DNA damage by adozelesin or 4NQO is clearly seen in a region of the 2D gel that is not obscured (Figure 4A). The level of X-structures is consistent with the level of origin activity and with our earlier finding that X-shaped sister chromatid junctions form at active ORI305 during the recombination-dependent bypass of DNA damage at the stalled fork (25). At the low level of proximal origin activity, passive replication of the mutated origin masks detection of fork stalling, but not the associated formation of a low level of sister chromatid junctions. Thus, detection of localized fork stalling at an origin is dependent on the level of proximal origin activity.

We also analyzed the ORI305 replicon for replication intermediates around naturally-inactive origins at *ARS304* near ORI305 and at the *ARS302*/*303*/*320* cluster near *HML* (16) on the left arm of chromosome III. These loci are telomeric to ORI305 and, in an unperturbed S phase, are replicated passively by a fork from the active origin (Figure 4B, map). G1–blocked cells were released synchronously into S phase in the absence or presence of adozelesin as in Figure 2, and replication intermediates were analyzed by 2D–gel electrophoresis. The passive replication of these loci in an unperturbed S phase was indicated by the presence of early–Y arcs and the absence of bubble arcs at 30, 45 and 60 min after release (Figure 4B, No DNA damage). The same was the case also in the presence of adozelesin, which, in contrast to its effect at active origin loci, did not induce prominent signals of localized fork stalling in the fragments containing the inactive origins (Figure 4B, Adozelesin). Some forks arrived synchronously at *ARS304* by 30 min, and later at the *ARS302*/*303*/*320* cluster. Progression of these forks appeared independent of the presence of the damaging agent, likely because they arose in a subpopulation of cells in which ORI305 had not yet reacted with adozelesin, which required >15 min and ≤ 30 min (Figure 2B). In other cells, however, ORI305 had reacted with the drug by 30 min and prominent fork stalling was induced (Figure 2B, 30 min). Weak fork pause signals detected at *ARS304* and *ARS302*/*303*/*320* were present in treated and untreated cells and likely result from dormant initiation protein complexes at these ARS elements which can exhibit inefficient origin activity in certain conditions (5,17,30). The faint X–structure signal at the *ARS304* fragment in the presence of adozelesin could result from a non-detectable level of origin activity at *ARS304*, similar to the case of the faint X-structure signal associated with the inefficient ORI305 activity at the *ARS305*–b5c7 locus, or possibly from limited branch migration of sister chromatid junctions formed at an adjacent origin. Forks began to clear and complete replication at *ARS304* by 60 min in the absence of DNA damage (Figure 4B), as did the replication intermediates at the active origin, ORI305 (Figure 2A). In contrast, in the presence of adozelesin, forks showed no signs of clearing at *ARS304* by 60 min (Figure 4B), nor did the replication intermediates at active ORI305 (Figure 2B). Together, the results indicate a general slowdown in fork progression in the ORI305 replicon and a persistence of localized stalling at the active origin.

The absence of prominent fork stalling induced by DNA damage at naturally-inactive origin sequences or at inactivated ORI305, both of which were replicated primarily by forks from distal origins, indicates that the detection of prominent localized fork stalling depends on proximal origin activity.

Localized fork stalling is not due to preferential DNA damage at an active origin versus inactive origins in a replicon

The dependence on proximal origin activity for localized fork stalling was unexpected, since it is generally assumed that all replication forks, whether proximal or distal to origins, respond in the same way upon encountering DNA damage. The result is not due to differences in the proximal and distal DNA sequences examined, since all yeast ARS elements, whether active or naturally inactive as chromosomal origins, contain AT–rich sequences (ca. 70% A+T over 150bp) and adozelesin reacts specifically with such sequences (24). Also, it is unlikely that the result is due to differences in chromatin structure at active and inactive origins since adozelesin reacts at similar sites in chromatin and in naked DNA (31). A possible explanation for the dependence on origin activity is that DNA alkylation by adozelesin is enhanced at active origin sequences as compared to similar replicon sequences that lack origin activity. Alternatively, DNA alkylation is the same at active and inactive origin sequences, but localized fork stalling in our conditions may occur primarily at bulky adducts proximal to active origins.

Upon exposure to high temperature, adozelesin DNA adducts create ssDNA nicks (32), which, when closely spaced on both DNA strands or situated opposite ssDNA gaps, generate DNA double–strand breaks. We tested the presence of adozelesin adducts by detecting double–strand break formation in replication intermediates at ORI305 and at the two naturally-inactive origin locations (*ARS304*, *ARS302*/*303*/*320*) within the ORI305

replicon. Control heating of replication intermediates at ORI305 from WT cells in unperturbed S phase resulted in no double-strand breaks (Figure 5A, panel 1). In contrast, replication intermediates at ORI305 from WT cells treated with adozelesin in S phase generated discrete double–strand breaks upon exposure to heat. The most frequent break points occurred in the center of the fragments (Figure 5A, panel 2), and mapped to the location of the active origin and the localized fork stalling. We obtained a similar result with a fragment containing active origin ORI508 (Supplementary Figure S3, panel 1). These findings imply that replication forks are stalled at origins by the DNA adducts at these sites. The presence of secondary off–centered break points within the ORI305 fragments indicates that adozelesin does not react exclusively near the origin initiation sites. To confirm that, we examined the regions containing naturally-inactive origins *ARS304* and *ARS302/303/320*, which, in WT cells, are passively replicated by forks emanating from ORI305 (Figure 5B, ORI305 replicon). Although adozelesin–dependent localized fork stalling was not detected in the proximity of these naturally-inactive origins (Figure 4B), multiple double–strand break sites were observed in the two genomic fragments upon heating (Figure 5A, panels 3 and 4), indicating the presence of DNA adducts.

Finally, we tested the presence of adducts in a fragment containing the inactivated ORI305 from cells harboring the *ARS305*–b5c7 point mutation. Remarkably, the break point pattern in the fragment containing the inactivated ORI305 was the same as that observed in the active ORI305 region (Figure 5A, panels 2 and 5), indicating a similar adduct distribution despite the lack of detectable localized fork stalling at the inactive origin (Figure 4A). The fragments containing naturally-inactive origins *ARS304* and *ARS302/303/320* also showed the same breakage pattern as in WT cells (Supplementary Figure S3, panels 2 and 3). Inactivation of ORI305 modifies the replicon organization and results in the passive replication of the region by forks generated at a distal active origin, ORI306 (Figure 5B, ORI306 replicon) (16). Taken together, these results show that the localized fork stalling and sister chromatid joining are not due to enhanced DNA alklyation at active origins compared to similar sequences that lack origin activity, but instead occur primarily at bulky adducts proximal to active origins.

Localized fork stalling is enhanced by the S–phase checkpoint at early origins and induced at late origins in checkpoint mutants

The presence of localized fork stalling at early–firing origin sites and its dependence on proximal origin activity as well as its occurrence in either direction imply that stalling takes place at a nearby DNA adduct encountered by a newly–formed replication fork, soon after origin firing. The persistence of localized stalling at the

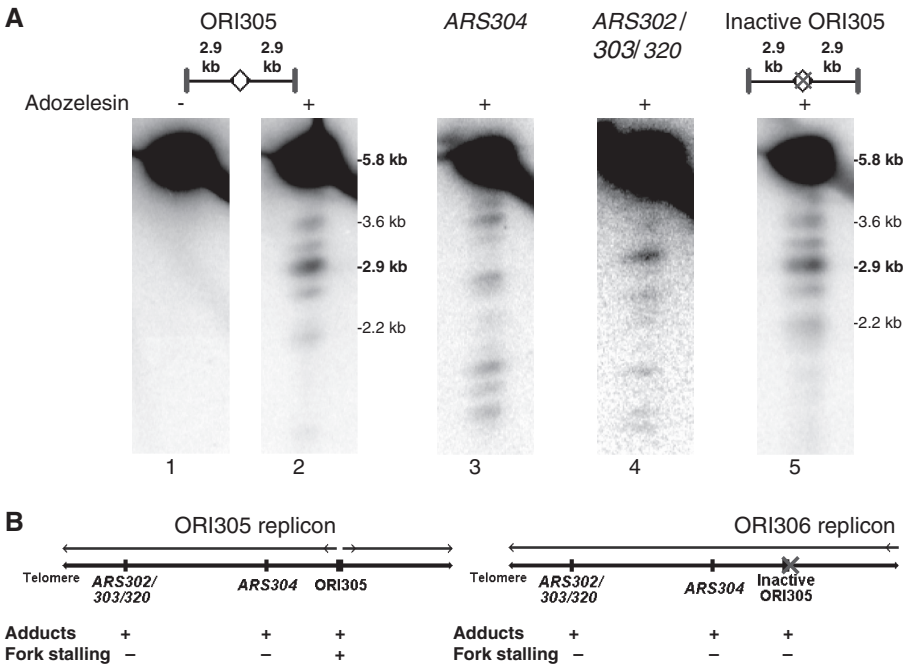

Figure 5. Heating of adozelesin-damaged DNA induces double-strand breaks at discrete sites. (**A**) G1–synchronized WT (panel 1–4) and *ARS305*–b5c7 mutant cells with inactive ORI305 (panel 5) were released into S phase in the presence of 1 μM adozelesin for 45 min and analyzed by 2D–gel electrophoresis. Replication intermediates were incubated in [10 mM Tris-HCl pH 7.9, 50 mM NaCl, 10 mM $MgCl_2$, 0.1 mM EDTA] for 4 h at 65°C between the first and second dimension electrophoresis. The molecular size of the degradation DNA bands from the full-length restriction fragment (1N spot) and the position of the origin site within the fragment for ORI305 are annotated. A control sample prepared similarly from WT cells in an unperturbed S phase is shown for ORI305. Results for ORI508 are in Supplementary Figure S3. (B) The direction of replication forks within the ORI305 and ORI306 replicons and the relation between the presence of adozelesin adducts as observed in (A) and the localized stalling at active origins is schematically represented in WT cells (active ORI305, left) or in cells with inactivated ORI305 (right). Results for *ARS304* and *ARS302/303/320* loci in cells with inactivated ORI305 are shown in Supplementary Figure S3.

origin over time and the general slowdown in fork progression in the replicon (Figure 2), as well as the lack of detectable stalling at DNA lesions elsewhere in the replicon (Figures 4 and 5) raise the possibility that the initial fork stalling includes a regulated step during the activation of a DNA damage response. A possible mechanism regulating the fork stalling at early origins is the intra–S–phase checkpoint, which is activated by the Mec1 sensor kinase, delays S-phase progression and is thought to allow time for DNA damage repair (33). To investigate the involvement of the checkpoint, we analyzed the replication intermediates during DNA damage in S phase in a *mec1*–100 mutant that is deficient in phosphorylating the Rad53 effector kinase and initiating the checkpoint response in S phase (27). The checkpoint-defective protein encoded by the *mec1*–100 mutant allele is still recruited at stalled forks and able to maintain sufficient replisome stability in the presence of DNA lesions to allow fork restart (12). After the release of *mec1*–100 cells from the G1 block into S phase in the presence of adozelesin, a fork stalling signal was still present at the sites of early origins ORI305 and ORI508, but its intensity relative to other replication intermediates was reduced at both origins compared to the relative level of fork stalling in WT cells (Figure 6). This suggests that, in the checkpoint mutant, replication forks remain stalled by DNA damage at active origin sites for shorter periods of time, which could contribute along with the late origin firing to the faster S–phase progression of *mec1*–100 cells compared to WT cells (Supplementary Figure S4). Results similar to those obtained using adozelesin were seen in the presence of 4NQO at both origins (Supplementary Figure S5). Ddc1, a component of the 9–1–1 checkpoint clamp, is recruited in parallel with Mec1 to stalled replication forks and is required for full Mec1 activation and initiation of the intra–S–phase checkpoint (8). We also observed a reduction in the relative level of the fork stalling signal and faster S–phase progression when *ddc1Δ* checkpoint mutant cells were released in the presence of adozelesin (Supplementary Figure S6). All of the results presented in this section indicate a role for the intra–S–phase checkpoint in enhancing the replication fork stalling caused by DNA damage at early origins in WT cells, possibly to allow time for DNA repair (33) or to facilitate fork resolution at subsequent lesions (see Discussion).

Late–firing origins have a delayed activation time in an unperturbed S phase compared to early origins, and their firing is inhibited in the presence of DNA damage by the intra–S–phase checkpoint (20,34). 2D–gel analysis of replication intermediates at late-firing ORI501 and ORI1412 in the absence of DNA damage revealed a bubble arc

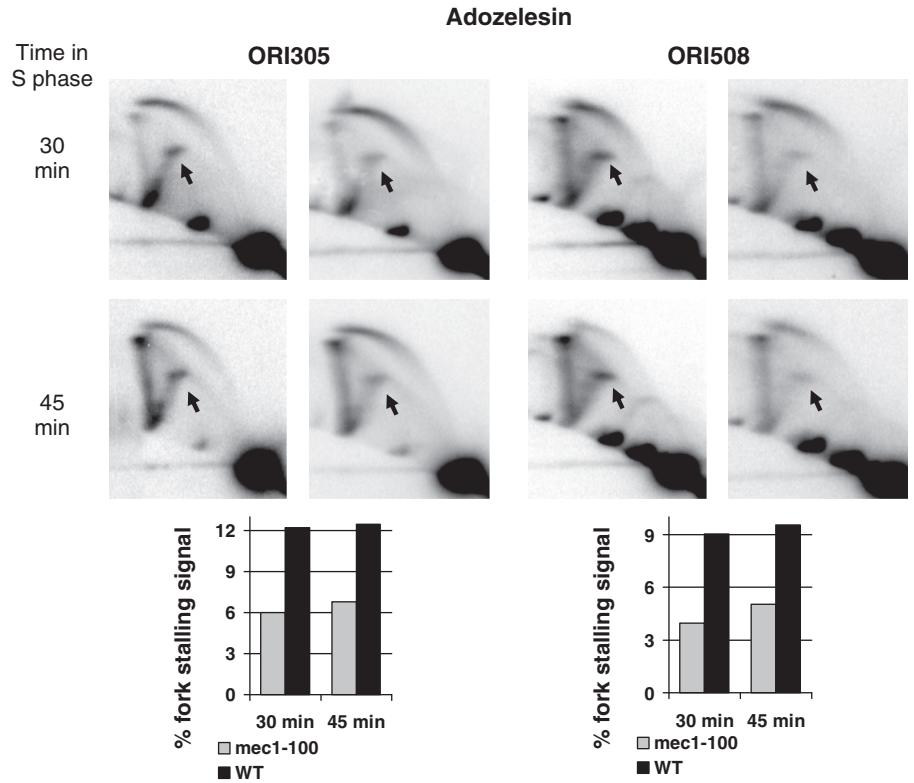

Figure 6. Inactivation of the intra–S–phase checkpoint diminishes damage–induced fork stalling at early–firing origins. G1–synchronized WT and *mec1*–100 cells were released into S phase in the presence of 1 μM adozelesin. Samples were taken for flow cytometry analysis (Supplementary Figure S4), and those collected at 30 and 45 min post–release for 2D–gel analysis of replication intermediates at early–firing origins ORI305 and ORI508 (WT, left panels for each ORI; *mec1*-100, right panels). The graphs show the fork–stalling signal intensity as a percentage of those of the replication intermediates in *mec1*–100 cells and separately in WT cells. Reduction in the relative fork stalling signal in the checkpoint mutant compared to that in WT cells was seen in three independent experiments, and also observed using 4NQO (Supplementary Figure S5), or using a *ddc1Δ* checkpoint mutant instead of *mec1*-100 (Supplementary Figure S6).

indicative of origin activity at 45 min after the G1–block release (Figure 7A). The faint X-DNA signal at ORI1412 represents transient hemicatenane structures that form in the absence of DNA damage (21). In the presence of adozelesin, the bubble–to–Y arc ratio decreased significantly at both origins, as expected for the inhibition of origin firing by the intra–S–phase checkpoint. The reduced intensity of the Y-arc signal at ORI1412 is due to minimal passive replication from flanking late origins (35) that are also subject to inhibition by the checkpoint. In these conditions, the fragments containing ORI501 and ORI1412 showed no localized fork stalling or chromatid junction signals (Figure 7A), further supporting an origin activity requirement for their induction.

Failure of intra–S–phase checkpoint activation during replication stress results in loss of inhibition of late origin firing, which still occurs later than early origin firing (20,34). The uncontrolled firing of late origins in the presence of DNA lesions could lead to localized fork stalling, as in the case of early origins. To test this, we analyzed replication intermediates at late ORI1412 in a variety of intra–S–phase checkpoint deficient strains released in S phase in the presence of adozelesin (Figure 7B). As expected, ORI1412 was activated in the *mec1*–100, *ddc1Δ*, *mrc1Δ* and *tof1Δ* checkpoint mutants, despite the presence of the DNA damaging agent. We found that the activation of the origin in these mutants was accompanied by localized fork stalling and sister chromatid joining (Figure 7B), unlike the situation in WT cells where late origin firing was inhibited by the intra–S–phase checkpoint (Figure 7A). Thus, localized fork stalling and sister chromatid joining caused by DNA damage can occur at a late origin in the absence of repression by the intra–S–phase checkpoint.

Taken together, these results show a differential effect of the intra–S–phase checkpoint on localized fork stalling at origins: on one hand, enhancing the fork arrest caused by DNA damage at early active origins, and, on the other hand, inhibiting the firing of late origins and subsequent stalling of replication forks at these sites. In addition, the results in checkpoint-defective mutants reveal a checkpoint-independent component of fork arrest caused by DNA damage at active early origins and at a de-repressed late origin.

DISCUSSION

DNA lesions constitute major obstacles for the progression of replication forks and pose a threat to genome integrity and cell survival. Despite its biological importance, little is known about the locations and determinants of replication fork stalling induced by DNA damage, and its consequences within cells are not fully understood. Here we found that, in budding yeast, bulky DNA damaging agents induce localized fork stalling at active replication origins, affecting forks moving in either direction, and that localized stalling is modulated by the intra-S-phase checkpoint. Additionally, localized fork stalling and the subsequent formation of sister chromatid junctions depended on proximal origin activity. Despite the formation of DNA adducts, localized fork stalling was abrogated by mutational inactivation of replication initiation and prominent stalling was not detected at naturally-inactive chromosomal origins. Intra–S–phase checkpoint inactivation diminished, but did not eliminate, fork stalling at early–firing origin sites, and induced localized stalling and chromatid joining at a de–repressed late–firing origin. Our results indicate that newly-created

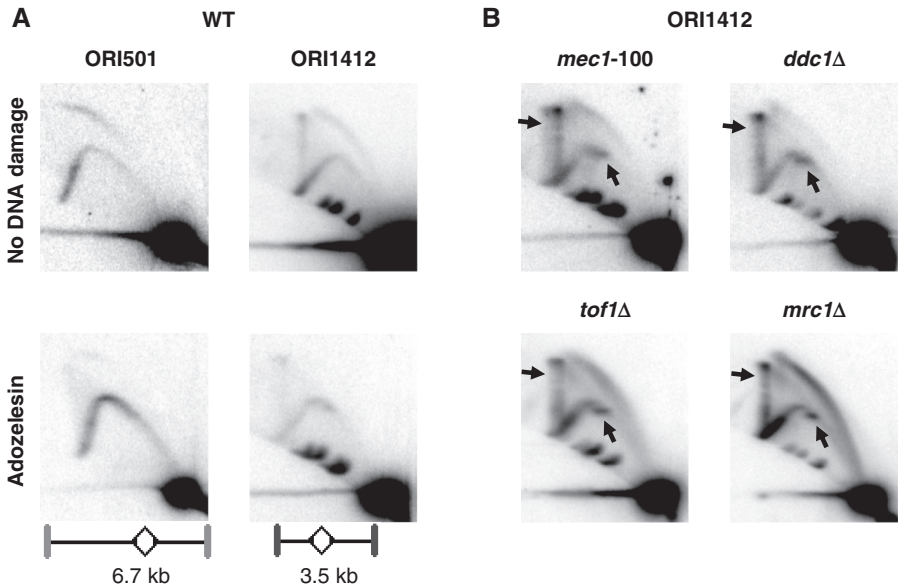

Figure 7. Inactivation of intra–S–phase checkpoint genes induces late origin firing, localized fork stalling and sister chromatid joining at ORI1412. (**A**) In control experiments, G1–synchronized WT cells were released into S phase without DNA damaging agents or in the presence of 1 μM adozelesin. Samples were collected at 45 min post–release for 2D–gel analysis of replication intermediates at late–firing origins ORI501 and ORI1412. (**B**) In checkpoint mutants *mec1*-100, *ddc1Δ*, *tof1Δ* and *mrc1Δ*, G1–synchronized cells were released into S phase in the presence of 1 μM adozelesin. Samples were collected at 45 min post–release for 2D–gel analysis of replication intermediates at late–firing origin ORI1412. The arrows indicate the X–shaped DNA structures and the fork–stalling signal induced in the checkpoint mutants.

forks encountering a bulky DNA adduct at active replication origins exhibit a dual nature of fork stalling: a checkpoint-independent arrest that triggers sister chromatid junction formation, as well as a checkpoint-enhanced arrest at early origins that accompanies the repression of late origin firing and may facilitate bypass and repair of subsequent lesions, as discussed below.

Localized fork stalling induced by DNA damage at active replication origins

Previously we reported that the DNA alkylating agent adozelesin induces fork stalling at an active replication origin, ORI305, in asynchronous cells incurring DNA damage in all phases of the cell cycle (17). ORI305 is activated early in S phase and, in the present work, we found that localized fork stalling occurs at several early–firing origins during S–phase DNA damage by adozelesin or a different agent, 4NQO. Although dissimilar in structure and chemical properties, both of these alkylating agents form bulky adducts in the minor groove of DNA which block the progression of DNA polymerases (36,37). 2D-gel analysis of replication intermediates is a highly sensitive method for detecting localized fork arrest, including weak fork pausing signals induced by DNA-bound proteins (5). However, for other types of commonly studied DNA damaging agents, localized fork stalling has not been previously detected using this technique. Widely studied UV–induced DNA damage, consisting mostly of intra–strand thymine dimers, is readily repaired by efficient nucleotide excision repair (NER) mechanisms, making necessary the use of NER mutants to investigate replication of DNA with UV lesions. In such mutants, persistent UV lesions slow down the replication fork progression and are bypassed through error–free translesion synthesis or gap formation and repair (19,38) without evidence of localized fork stalling (19,22). MMS, another frequently used DNA damaging agent, induces methylation of purine nucleotides which is counteracted by base excision repair mechanisms (39). The replicative bypass of MMS lesions is not well understood, but unlike UV–lesion bypass, it does not seem to involve gap formation (19). MMS lesions also slow down replication fork progression in WT cells (18) and, like UV lesions, do not induce localized fork stalling (20,21) (Supplementary Figure S1).

Although adozelesin has an affinity for AT–rich sequences, which are present at all budding yeast replication origins, we provided evidence that it reacts widely with DNA, and not only at active replication origins. There is no reported sequence specificity for 4NQO, and we envisage that it also forms widely distributed DNA adducts. Surprisingly, prominent localized fork stalling followed by sister chromatid joining occurred only at early–firing origins in WT cells and was not detected in passively-replicated regions containing inactive origins, despite the presence of similar AT content. In addition to the dependence on origin activity, the localized stalling involved forks generated proximally and moving in either direction from the active origin, but not forks incoming from distal origins. These results imply that a major stalling site is created at the origin when a newly–formed replication fork encounters the first bulky adduct on the DNA template. Minor stalling sites, which sometimes occur elsewhere in the large restriction fragments (4600–7500 bp) containing the centrally-located origin (~150 bp), likely arise in a subpopulation of cells lacking DNA damage at the origin. The forks involved in localized stalling were generated at origins that fire early in S–phase in WT cells, and at late origins in checkpoint mutants that de-repress late origin firing. Thus, it is the origin activity and the first encounter of a newly-created fork with a DNA lesion, not simply the early firing, that leads to localized fork stalling by bulky DNA adducts at replication origins.

We found that one cellular response activated by the presence of bulky DNA adducts during replication, the intra–S–phase checkpoint, enhances the localized fork stalling. In S–phase checkpoint mutants, the damage–induced localized fork stalling is present, although diminished, at early origins. Furthermore, the sister chromatid junctions that arise after localized fork stalling at active origins formed independently of the intra–S–phase checkpoint, both at late and early origins. Elsewhere we found that sister chromatid junction formation is recombination dependent and critical for resolving replication forks stalled by adozelesin DNA damage and for completing chromosome duplication (25). Here, prominent localized fork stalling and sister chromatid junctions were not detected at replicon sequences downstream from active origins. As one possibility, these results could suggest that the Mec1-enhanced fork arrest provides time for DNA repair, as originally proposed based on the checkpoint slowing of S phase (33). Genetic analysis indicates involvement of nucleotide excision repair following adozelesin damage, however, that pathway is separate from the error-free damage bypass pathway that resolves the initial localized fork stalling through sister chromatid junction formation (25). Recently, the Mec1 kinase was found to mediate a key interaction at replication forks stalled by DNA damage, by phosphorylating and activating Slx4 in a scaffold protein complex that recruits fork repair factors (40). *SLX4* also interacts with error-free damage bypass genes, and the *slx4Δ* mutant, like the *rad5Δ* damage bypass mutant deficient in replication fork recombination (25), is unable to complete DNA replication after fork stalling (41). Finally, the Slx4 ortholog in several other eukaryotes functions as a subunit of a Holliday junction resolvase (42), an activity that would permit sister chromatid junction separation following Rad5-mediated damage bypass (25). Thus, in addition to possibly providing time for repair, the Mec1-enhanced fork arrest localized at the initial DNA damage encounter may involve formation of such a scaffold protein complex to facilitate error-free bypass and subsequent repair at downstream lesions.

Stalling at active origin sites affects fork progression in either direction

The resolution of 2D–gel analysis of replication intermediates indicates that the damage–induced localized fork

stalling maps inside a ~500 bp region which contains the ~150 bp DNA elements that comprise an active origin (14). The nature of the replication intermediates indicates that, after bidirectional origin firing, one fork is stalled in close proximity of the origin, while the opposite fork is not stalled and able to progress outside the studied restriction fragment. We found that either fork can be blocked near the origin site under our conditions. However, it is possible that, due to sequence differences in the sites of adduct formation, the stalling could occur mainly in one direction at particular origins or with certain damaging agents. In this regard the intensity of the fork stalling signals on the early–Y arc can differ between the two 'asymmetrical' restriction digests used to assess the fork block direction.

While only one of the two forks appears to be blocked at each origin, we did not detect prominent localized stalling at forks that progressed outside the origin-containing fragment and through the replicon. However, following DNA damage bypass at the origin (25), the overall slowing of fork movement we detected in the replicon may reflect events that facilitate fork resolution at subsequent lesions as discussed above. Also, the checkpoint-enhanced stalling of one fork might coordinate the bypass and repair mechanisms to protect both forks in the replicon from subsequent stalling since the two newly–formed replication forks can remain in contact within replication factories (43) or in DNA damage–induced foci (44).

We can not exclude the possibility that in rare instances, or in different conditions such as extremely high levels of DNA damage, both newly-established forks in a replicon are blocked by the first lesion encounter near the active origin site. The minuscule bubble formed in these cases would be impossible to detect by 2D–gel analysis due to overlap with the intense 1N spot.

Intra–S–phase checkpoint influence on DNA damage–induced fork stalling

DNA damage induced by MMS activates the intra–S–phase checkpoint (20,33), and so does that induced by bulky adducts as indicated here by the slowing of S–phase progression (Figure 2), and the inhibition of late–firing origins (Figure 7A). Whereas slowing of fork progression in the presence of MMS damage appears independent of S-phase checkpoint activation (18), and deactivation of the Rad53 checkpoint kinase during recovery in the absence of MMS is required to restore the rate of progression (45), the checkpoint effect on localized fork stalling was not clear. In an earlier report (17), the adozelesin–induced fork stalling at active origin ORI305 in asynchronous cells did not appear to be influenced by the inactivation of checkpoint proteins Mec1 or Rad53 using null alleles. However, the absence of Mec1 and Rad53 influences the stability of stalled replication forks and can lead to replisome collapse or fork breakage (8). Here we used synchronized cells exposed to DNA damage in S phase and a separation–of–function *mec1*–100 mutant, which is defective in activating the effector kinase Rad53 and inducing a checkpoint response during S phase, but maintains the replisome stability in the presence of DNA damage (12,27). We also used a *ddc1Δ* mutant which has an S–phase checkpoint defect due to inefficient activation of Mec1 (9). Unlike *mec1* null mutants, the *mec1*–100 mutant is only mildly sensitive to DNA damaging agents (27), including adozelesin (data not shown), but has a high rate of hydroxyurea–induced gross chromosomal rearrangements, possibly due to uncontrolled recombination events during replication stalling (46). We found that inactivation of intra–S–phase checkpoint signaling in *mec1*–100 and *ddc1Δ* reduces, but does not eliminate, the fork stalling at active origin sites. The shorter time of fork stalling could contribute, along with the late origin firing, to the faster S–phase progression observed in *mec1*–100 and *ddc1Δ* mutants as compared to WT cells (Supplementary Figures S4 and S6).

Previous studies showed that DNA damage bypass and S–phase checkpoint mechanisms are activated independently but by common intermediates at stalled replication forks (47). Consistent with this, our results suggest a dual nature of the fork stalling at the first replication-blocking lesion: a checkpoint-independent fork arrest that induces sister chromatid junction formation, shown elsewhere to require DNA damage bypass and recombination mechanisms (25), and an enhanced fork arrest that requires the intra-S-phase checkpoint. While the latter is not essential for DNA replication in the presence of damage, it could represent a control pathway for error-free bypass and repair, as well as for preventing unscheduled or inaccurate fork restart events that could lead to mutations or chromosomal rearrangements.

In addition to reducing the damage–induced fork stalling at early active origins, the inactivation of intra–S–phase checkpoint induced the firing and fork stalling at a late replication origin. Tof1 and Mrc1 are replisome components required for full intra–S–phase checkpoint activation and for the stabilization of replication forks stalled by nucleotide depletion (48). Tof1 also regulates the programmed fork pausing at protein–induced replication fork barriers (4). We found that the DNA damage–induced fork stalling does not require Mrc1 or Tof1, as the absence of these factors in the corresponding mutants induced firing and fork stalling at a late origin (Figure 7B) and had an insignificant influence on fork stalling at early origins (data not shown). These results indicate that the regulation of fork stalling at sites of bulky DNA damage differs from that induced by nucleotide depletion or by DNA–bound proteins at natural replication fork barriers. Additionally, unlike the localized fork stalling induced by bulky DNA adducts characterized here and the requirements for damage bypass and sister chromatid junction formation identified elsewhere (25), replication forks paused at natural replication fork barriers do not activate the intra–S–phase checkpoint and do not require recombination mechanisms to restart replication (4).

Our findings provide new insights into how cells handle the replication of DNA damaged by bulky alkylating agents, with forks that arise at active origins arresting locally, at a proximal lesion encounter, leading to checkpoint-independent sister chromatid junction

formation as well as checkpoint-enhanced fork stalling at early origins that accompanies repression of late origin firing and may facilitate lesion bypass and repair. Further investigation of DNA damage–induced fork stalling and restart mechanisms in model organisms like budding yeast can offer important clues about conserved processes in higher eukaryotes including humans, and about their implications in genetic instability and cancer.

FUNDING

National Institutes of Health (grant GM30614 to D.K.); Roswell Park Cancer Institute, National Cancer Institute grant (CA016056). Funding for open access charge: Departmental funds.

Conflict of interest statement. None declared.

REFERENCES

1. Myung,K. and Kolodner,R.D. (2002) Suppression of genome instability by redundant S-phase checkpoint pathways in Saccharomyces cerevisiae. *Proc. Natl Acad. Sci. USA*, **99**, 4500–4507.
2. Barbour,L. and Xiao,W. (2003) Regulation of alternative replication bypass pathways at stalled replication forks and its effects on genome stability: a yeast model. *Mutat. Res.*, **532**, 137–155.
3. Ivessa,A.S., Lenzmeier,B.A., Bessler,J.B., Goudsouzian,L.K., Schnakenberg,S.L. and Zakian,V.A. (2003) The Saccharomyces cerevisiae helicase Rrm3p facilitates replication past nonhistone protein-DNA complexes. *Mol. Cell*, **12**, 1525–1536.
4. Calzada,A., Hodgson,B., Kanemaki,M., Bueno,A. and Labib,K. (2005) Molecular anatomy and regulation of a stable replisome at a paused eukaryotic DNA replication fork. *Genes Dev.*, **19**, 1905–1919.
5. Wang,Y., Vujcic,M. and Kowalski,D. (2001) DNA replication forks pause at silent origins near the HML locus in budding yeast. *Mol. Cell. Biol.*, **21**, 4938–4948.
6. Merchant,A.M., Kawasaki,Y., Chen,Y., Lei,M. and Tye,B.K. (1997) A lesion in the DNA replication initiation factor Mcm10 induces pausing of elongation forks through chromosomal replication origins in Saccharomyces cerevisiae. *Mol. Cell. Biol.*, **17**, 3261–3271.
7. Lambert,S. and Carr,A.M. (2005) Checkpoint responses to replication fork barriers. *Biochimie*, **87**, 591–602.
8. Friedel,A.M., Pike,B.L. and Gasser,S.M. (2009) ATR/Mec1: coordinating fork stability and repair. *Curr. Opin. Cell Biol.*, **21**, 237–244.
9. Majka,J., Niedziela-Majka,A. and Burgers,P.M. (2006) The checkpoint clamp activates Mec1 kinase during initiation of the DNA damage checkpoint. *Mol. Cell*, **24**, 891–901.
10. Tourriere,H. and Pasero,P. (2007) Maintenance of fork integrity at damaged DNA and natural pause sites. *DNA Repair*, **6**, 900–913.
11. Chang,D.J. and Cimprich,K.A. (2009) DNA damage tolerance: when it's OK to make mistakes. *Nat. Chem. Biol.*, **5**, 82–90.
12. Tercero,J.A., Longhese,M.P. and Diffley,J.F. (2003) A central role for DNA replication forks in checkpoint activation and response. *Mol. Cell*, **11**, 1323–1336.
13. Bell,S.P. and Dutta,A. (2002) DNA replication in eukaryotic cells. *Annu. Rev. Biochem.*, **71**, 333–374.
14. Aladjem,M.I., Falaschi,A. and Kowalski,D. (2006) In DePamphillis,M.L. (ed.), *DNA Replication and Human Disease*. Cold Spring Harbor Laboratory Press, Cold Spring Harbor, NY, pp. 31–61.
15. Donaldson,A.D. and Schildkraut,C.L. (2006) In DePamphillis,M.L. (ed.), *DNA Replication and Human Disease*. Cold Spring Harbor Laboratory Press, Cold Spring Harbor, NY, pp. 197–215.
16. Vujcic,M., Miller,C.A. and Kowalski,D. (1999) Activation of silent replication origins at autonomously replicating sequence elements near the HML locus in budding yeast. *Mol. Cell. Biol.*, **19**, 6098–6109.
17. Wang,Y., Beerman,T.A. and Kowalski,D. (2001) Antitumor drug adozelesin differentially affects active and silent origins of DNA replication in yeast checkpoint kinase mutants. *Cancer Res.*, **61**, 3787–3794.
18. Tercero,J.A. and Diffley,J.F. (2001) Regulation of DNA replication fork progression through damaged DNA by the Mec1/Rad53 checkpoint. *Nature*, **412**, 553–557.
19. Lopes,M., Foiani,M. and Sogo,J.M. (2006) Multiple mechanisms control chromosome integrity after replication fork uncoupling and restart at irreparable UV lesions. *Mol. Cell*, **21**, 15–27.
20. Shirahige,K., Hori,Y., Shiraishi,K., Yamashita,M., Takahashi,K., Obuse,C., Tsurimoto,T. and Yoshikawa,H. (1998) Regulation of DNA-replication origins during cell-cycle progression. *Nature*, **395**, 618–621.
21. Lopes,M., Cotta-Ramusino,C., Liberi,G. and Foiani,M. (2003) Branch migrating sister chromatid junctions form at replication origins through Rad51/Rad52-independent mechanisms. *Mol. Cell*, **12**, 1499–1510.
22. Neecke,H., Lucchini,G. and Longhese,M.P. (1999) Cell cycle progression in the presence of irreparable DNA damage is controlled by a Mec1- and Rad53-dependent checkpoint in budding yeast. *EMBO J.*, **18**, 4485–4497.
23. Swenson,D.H., Li,L.H., Hurley,L.H., Rokem,J.S., Petzold,G.L., Dayton,B.D., Wallace,T.L., Lin,A.H. and Krueger,W.C. (1982) Mechanism of interaction of CC-1065 (NSC 298223) with DNA. *Cancer Res.*, **42**, 2821–2828.
24. Lee,C.S., Pfeifer,G.P. and Gibson,N.W. (1994) Mapping of DNA alkylation sites induced by adozelesin and bizelesin in human cells by ligation-mediated polymerase chain reaction. *Biochemistry*, **33**, 6024–6030.
25. Minca,E.C. and Kowalski,D. (2010) Multiple Rad5 activities mediate sister chromatid recombination to bypass DNA damage at stalled replication forks. *Mol. Cell*, **38**, 649–661.
26. Huang,R.Y. and Kowalski,D. (1993) A DNA unwinding element and an ARS consensus comprise a replication origin within a yeast chromosome. *EMBO J.*, **12**, 4521–4531.
27. Paciotti,V., Clerici,M., Scotti,M., Lucchini,G. and Longhese,M.P. (2001) Characterization of mec1 kinase-deficient mutants and of new hypomorphic mec1 alleles impairing subsets of the DNA damage response pathway. *Mol. Cell. Biol.*, **21**, 3913–3925.
28. Benard,M., Maric,C. and Pierron,G. (2001) DNA replication-dependent formation of joint DNA molecules in Physarum polycephalum. *Mol. Cell*, **7**, 971–980.
29. Dijkwel,P.A., Vaughn,J.P. and Hamlin,J.L. (1991) Mapping of replication initiation sites in mammalian genomes by two-dimensional gel analysis: stabilization and enrichment of replication intermediates by isolation on the nuclear matrix. *Mol. Cell. Biol.*, **11**, 3850–3859.
30. Szyjka,S.J., Viggiani,C.J. and Aparicio,O.M. (2005) Mrc1 is required for normal progression of replication forks throughout chromatin in S. cerevisiae. *Mol. Cell*, **19**, 691–697.
31. McHugh,M.M., Woynarowski,J.M., Mitchell,M.A., Gawron,L.S., Weiland,K.L. and Beerman,T.A. (1994) CC-1065 bonding to intracellular and purified SV40 DNA: site specificity and functional effects. *Biochemistry*, **33**, 9158–9168.
32. Reynolds,V.L., Molineux,I.J., Kaplan,D.J., Swenson,D.H. and Hurley,L.H. (1985) Reaction of the antitumor antibiotic CC-1065 with DNA. Location of the site of thermally induced strand breakage and analysis of DNA sequence specificity. *Biochemistry*, **24**, 6228–6237.
33. Paulovich,A.G. and Hartwell,L.H. (1995) A checkpoint regulates the rate of progression through S phase in S. cerevisiae in response to DNA damage. *Cell*, **82**, 841–847.
34. Santocanale,C. and Diffley,J.F. (1998) A Mec1- and Rad53-dependent checkpoint controls late-firing origins of DNA replication. *Nature*, **395**, 615–618.

35. Friedman,K.L., Diller,J.D., Ferguson,B.M., Nyland,S.V., Brewer,B.J. and Fangman,W.L. (1996) Multiple determinants controlling activation of yeast replication origins late in S phase. *Genes Dev.*, **10**, 1595–1607.
36. Sun,D. and Hurley,L.H. (1992) Effect of the (+)-CC-1065-(N3-adenine)DNA adduct on in vitro DNA synthesis mediated by Escherichia coli DNA polymerase. *Biochemistry*, **31**, 2822–2829.
37. Panigrahi,G.B. and Walker,I.G. (1990) The N2-guanine adduct but not the C8-guanine or N6-adenine adducts formed by 4-nitroquinoline 1-oxide blocks the 3′-5′ exonuclease action of T4 DNA polymerase. *Biochemistry*, **29**, 2122–2126.
38. Johnson,R.E., Prakash,S. and Prakash,L. (1999) Efficient bypass of a thymine-thymine dimer by yeast DNA polymerase, Poleta. *Science*, **283**, 1001–1004.
39. Vazquez,M.V., Rojas,V. and Tercero,J.A. (2008) Multiple pathways cooperate to facilitate DNA replication fork progression through alkylated DNA. *DNA Repair*, **7**, 1693–1704.
40. Ohouo,P.Y., Bastos de Oliveira,F.M., Almeida,B.S. and Smolka,M.B. (2010) DNA damage signaling recruits the Rtt107-Slx4 scaffolds via Dpb11 to mediate replication stress response. *Mol. Cell*, **39**, 300–306.
41. Flott,S., Alabert,C., Toh,G.W., Toth,R., Sugawara,N., Campbell,D.G., Haber,J.E., Pasero,P. and Rouse,J. (2007) Phosphorylation of Slx4 by Mec1 and Tel1 regulates the single-strand annealing mode of DNA repair in budding yeast. *Mol. Cell. Biol.*, **27**, 6433–6445.
42. Svendsen,J.M. and Harper,J.W. (2010) GEN1/Yen1 and the SLX4 complex: solutions to the problem of Holliday junction resolution. *Genes Dev.*, **24**, 521–536.
43. Kitamura,E., Blow,J.J. and Tanaka,T.U. (2006) Live-cell imaging reveals replication of individual replicons in eukaryotic replication factories. *Cell*, **125**, 1297–1308.
44. Lisby,M. and Rothstein,R. (2004) DNA damage checkpoint and repair centers. *Curr. Opin. Cell Biol.*, **16**, 328–334.
45. Szyjka,S.J., Aparicio,J.G., Viggiani,C.J., Knott,S., Xu,W., Tavare,S. and Aparicio,O.M. (2008) Rad53 regulates replication fork restart after DNA damage in Saccharomyces cerevisiae. *Genes Dev.*, **22**, 1906–1920.
46. Cobb,J.A., Schleker,T., Rojas,V., Bjergbaek,L., Tercero,J.A. and Gasser,S.M. (2005) Replisome instability, fork collapse, and gross chromosomal rearrangements arise synergistically from Mec1 kinase and RecQ helicase mutations. *Genes Dev.*, **19**, 3055–3069.
47. Davies,A.A., Huttner,D., Daigaku,Y., Chen,S. and Ulrich,H.D. (2008) Activation of ubiquitin-dependent DNA damage bypass is mediated by replication protein a. *Mol. Cell*, **29**, 625–636.
48. Katou,Y., Kanoh,Y., Bando,M., Noguchi,H., Tanaka,H., Ashikari,T., Sugimoto,K. and Shirahige,K. (2003) S-phase checkpoint proteins Tof1 and Mrc1 form a stable replication-pausing complex. *Nature*, **424**, 1078–1083.